Article published online: 2026-02-24

Original Article

# Quantitative Ultrasound As an Alternative Method for Assessment and Grading of Hepatic Steatosis: A Comparison Study with Quantitative MRI-Proton Density Fat Fraction

Thi Duyen Nguyen[1] Ngoc Thanh Hoang[1] Thi Ngoc Ha Hoang[1] Trong Binh Le[1] Thanh Thao Nguyen[1]

[1] Department of Radiology, University of Medicine and Pharmacy, Hue University, Hue, Vietnam

Indian J Radiol Imaging

**Address for correspondence** Thanh Thao Nguyen, MD, PhD, Department of Radiology, University of Medicine and Pharmacy, Hue University, 06 Ngo Quyen, Hue 53000, Vietnam (e-mail: ntthao@hueuni.edu.vn).

## Abstract

**Purpose** Although liver biopsy remains the gold standard for diagnosis of hepatic steatosis, non-invasive imaging is essential for population screening, risk assessment, and monitoring treatment. New ultrasonic techniques enable quantitative assessment of steatosis in individuals with hepatic metabolic disorders, offering an alternative noninvasive screening method. This study aims to evaluate the diagnostic accuracy of quantitative ultrasound fat fraction (USFF) in detecting and grading hepatic steatosis, using quantitative magnetic resonance imaging-proton density fat fraction (MRI-PDFF) as the reference standard.

**Materials and Methods** In this single-center prospective study (January 2024–July 2025), 40 consecutive adults (average age 57.83 ± 15.7 years; 14 men) referred for liver fat measurement underwent multivariable quantitative ultrasound (Samsung V7, convex probe CA 1–7 MHz) and 1.5-T MRI within 24 hours. After fasting for at least 4 hours, five reliable ultrasound acquisitions (reliability index $R^2 \geq 0.60$) of tissue attenuation imaging (TAI) and tissue scatter-distribution imaging (TSI) were obtained through a right intercostal window, and their means were automatically converted to USFF (%). MRI-PDFF maps were created using a six-echo spoiled gradient-echo sequence with multi-peak fat modeling and T2* correction. Steatosis grades were classified on USFF and PDFF as S0 (0–5%), S1 ($\geq$ 5%), S2 ($\geq$ 15%), and S3 (>25%). Pearson correlation and weighted $\kappa$ statistics were used for analysis (SPSS v20).

**Results** MRI-PDFF classified 15/40 (37.5%) of the livers as S0, 19/40 (47.5%) as S1, 3/40 (7.5%) as S2, and 3/40 (7.5%) as S3. The corresponding USFF distribution was S0 for 8/40 (20%), S1 for 19/40 (47.5%), S2 for 8/40 (20%), and S3 for 5/40 (12.5%). USFF showed a strong correlation with MRI-PDFF ($r = 0.912$; 99% CI 0.805–0.961; $p < 0.001$).

**Keywords**
- quantitative ultrasound
- ultrasound fat fraction
- proton density fat fraction
- MRI
- hepatic steatosis
- echo times

**DOI** https://doi.org/10.1055/s-0046-1817156.
**ISSN** 0971-3026.



Thieme Medical and Scientific Publishers Pvt. Ltd., A-12, 2nd Floor, Sector 2, Noida-201301 UP, India

**Conclusion** Quantitative ultrasound shows excellent correlation and strong agreement with MRI-PDFF for both detection and grading of hepatic steatosis. Given its low cost, real-time capability, and wide availability, USFF is a practical alternative for routine assessment and ongoing monitoring of hepatic fat.

## Introduction

The global prevalence of hepatic steatosis has increased rapidly due to sedentary lifestyles, obesity, and metabolic syndrome.[1] Without early detection, simple steatosis can advance to steatohepatitis, fibrosis, cirrhosis, and hepatocellular carcinoma.[2] Although liver biopsy remains the gold standard for diagnosis, non-invasive imaging is essential for population screening, risk assessment, and monitoring treatment.[3]

B-mode ultrasonography is affordable and widely accessible but remains subjective.[4] Computed tomography relies on ionizing radiation, while magnetic resonance imaging proton density fat fraction (MRI-PDFF), currently serves as the non-invasive gold standard for quantitative fat measurement. However, they are expensive and not available everywhere.[5] Multivariable quantitative ultrasound (QUS), which combines tissue attenuation and backscatter metrics, has become a quick method for estimating liver fat as a percentage, known as ultrasound fat fraction (USFF).[6] We prospectively assessed the diagnostic value of USFF compared with magnetic resonance imaging-proton density fat fraction (MRI-PDFF).

## Materials and Methods

### Study Design and Population

This cross-sectional study was approved by the institutional research ethics committee. Forty adults ($\geq$18 years) scheduled for liver fat quantification between January 2024 and July 2025 were enrolled. Exclusion criteria included (1) focal hepatic lesion, (2) prior hepatic surgery or intervention, (3) substantial alcohol consumption, and (4) chronic liver disorders other than steatosis.

### Quantitative Ultrasound Protocol

All examinations were performed after at least 4 hours of fasting, using a Samsung V7 scanner with a 1 to 7 MHz convex transducer. The examiners were blinded to the MRI-PDFF quantitative results. Following a standard B-mode survey, QUS measurements were taken in segments V to VI through a right intercostal window with the patient lying supine and the right arm abducted. A $2 \times 3$ cm fan-shaped ROI, positioned approximately 2 cm below the liver capsule and avoiding large vessels, was used. Five consecutive acquisitions, each with a reliability index $R^2 \geq 0.60$, were performed; their mean values for tissue attenuation imaging (TAI) and tissue scatter-distribution imaging (TSI) were automatically converted to USFF (%) following the equation used by Jeon et al[4]

$$\text{USFF} = -44.3 + 41.9 \times \text{TAI} + 0.23 \times \text{TSI}$$

### MRI Acquisition and PDFF Quantification

Quantitative MRI served as the reference standard for measuring fat fraction. Patients were scanned in the supine position using a 1.5-Tesla MRI system (Amira, Siemens Healthineers) with a 13-channel phased-array torso coil centered over the liver. Imaging involved a multi-echo gradient echo (ME-GRE) sequence acquired during a single breath-hold, covering the entire liver in the axial plane. A body coil was used with auto-selection disabled, and the ME-GRE sequence was performed without fat saturation. To reduce T1 contrast, the repetition time was set to 139 ms and the flip angle (FA) to 20 degrees, with echo times (TEs) as multiples of 1.2 ms.[7,8] Multiple echoes were acquired at TEs when fat and water signals are often in-phase or out-of-phase. The bandwidth was adjusted to achieve the desired TEs. One excitation was used, with imaging conducted in the axial plane. The number of slices was set to 10 to accommodate 12 TEs, with a slice thickness of 7 mm and a 20% gap. An asymmetric matrix ($128 \times 102$) was used to shorten acquisition time. Phase encoding was in the anterior–posterior direction, with a field of view of 40 cm and an estimated acquisition time of 12 seconds. The radiologist and radiographer initially reviewed the image quality to verify its suitability for quantitative analysis. Cases with artifacts, such as respiratory motion or susceptibility artifacts affecting the region of interest, were excluded from the study.

ME-GRE magnitude images were processed using a freely available research software called MRQuantif (http://imagemed.univ-rennes1.fr/mrquantif). MRQuantif provides scientifically validated quantification of hepatic iron and fat from a gradient-echo sequence.[8] Three non-overlapping circular regions of interest (ROIs) in the right hepatic lobe (segments V and VI) on the multi-echo sequence images, each measuring $\leq 5\,\text{cm}^2$, were selected. Care was taken to avoid large vessels, bile ducts, liver edges, focal hepatic lesions, and imaging artifacts.[1,6,9] These ROIs correspond to the quantitative locations of ROIs on ultrasound. Additionally, two ROIs were placed in the paraspinal muscles, and one ROI was positioned outside the body to measure background noise.[10] These ROIs will be transferred to all images, maintaining the exact location but with different TE. The placement of each ROI is shown in ►**Fig. 1**. The mean PDFF for each ROI within the liver parenchyma was recorded, and the

 

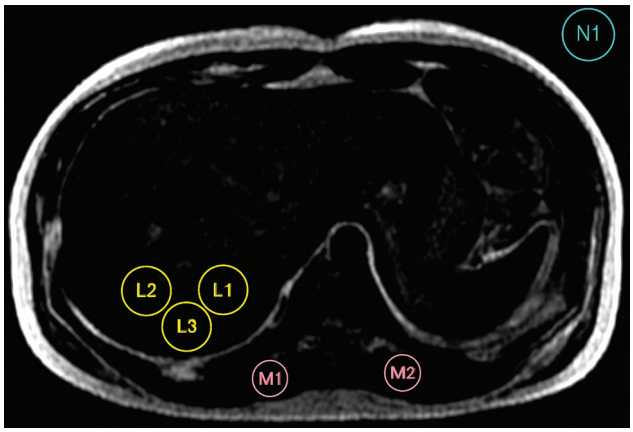


**Fig. 1** The placement of ROIs in MRI-PDFF (L1, L2, L3 for liver; M1, M2 for paraspinal muscle; N1 for background noise). MRI-PDFF, magnetic resonance imaging-proton density fat fraction; ROI, regions of interest.

overall liver fat content was calculated as the average of the three measurements.[9,11] Quantitative ROIs were manually placed by a board-certified radiologist and a senior radiology resident to ensure consistency and accuracy.

### USFF and MRI PDFF Cut-offs

Steatosis grades were defined using the following thresholds for both USFF and MRI-PDFF: S0: <5%, S1: ≥5%, S2: ≥15%, S3: ≥25%.

### Statistical Analysis

Statistical analysis was performed using SPSS v20.0. Continuous variables (age, MRI-PDFF, USFF) were tested for normality with the Shapiro–Wilk test and reported as mean ± SD, while categorical data were shown as counts and percentages. The linear relationship between USFF and MRI-PDFF was evaluated using Pearson's correlation coefficient; a two-sided *p*-value of <0.05 and a 99% confidence interval (CI) for *r* were used to address multiple comparisons in a small sample. Receiver operating characteristic (ROC) curve analysis assessed USFF's ability to detect any hepatic steatosis (MRI-PDFF ≥ 5%), moderate steatosis (MRI-PDFF ≥ 15%), and severe steatosis (MRI-PDFF ≥ 25%). Pairwise comparisons of the areas under the ROC curves (AUCs) between USFF and TAI or USFF and TSI were made using the DeLong test. For exploratory dichotomous analysis (normal liver vs. ≥S1 steatosis), the sensitivity, specificity, positive and negative predictive values, and overall accuracy at a USFF threshold of ≥5% were calculated with 95% CIs via the Wilson method. No missing data or severe outliers were found, so all 40 exams were included in the final analysis.

## Results

### Patient Characteristics

Forty patients (14 men and 26 women) were analyzed; the average age was 57.8 ± 15.7 years, ranging from 22 to 83 years, and the average body mass index was 23.5 ± 1.9 kg/m$^2$.

### Hepatic Fat Fraction Measured by MRI-PDFF and USFF

The mean USFF for the entire cohort was 11.8 ± 8.4%. Mean MRI-PDFF was 9.1 ± 8.6%.

Distribution of steatosis grades is summarized in ►**Table 1**.

USFF classified 8 out of 40 (20%) as S0, 19 out of 40 (47.5%) as S1, 8 out of 40 (20%) as S2, and 5 out of 40 (12.5%) as S3.

MRI-PDFF classified 15 out of 40 (37.5%) livers as S0, 19 out of 40 (47.5%) as S1, 3 out of 40 (7.5%) as S2, and 3 out of 40 (7.5%) as S3.

### Diagnostic Performance of QUS Parameters and Multivariable Fat Fraction Estimator for Hepatic Steatosis

We assessed the diagnostic performance of TAI, TSI, and USFF derived from a multivariable regression model to evaluate hepatic steatosis. Among the three parameters, USFF showed the highest AUC for detecting MRI-PDFF ≥ 5%, ≥15%, and ≥25% (AUCs of 0.915, 0.995, and 0.991, respectively; ►**Fig. 2**).

### Correlation Analysis

USFF showed a strong correlation with MRI-PDFF ($r = 0.912$; 99% CI, 0.805–0.961; $p < 0.001$; ►**Fig. 3**).

### Diagnostic Accuracy for the Presence of Steatosis (≥S1)

For diagnosing hepatic steatosis (MRI-PDFF ≥ 5%), the cutoffs of USFF were 9.14% sensitivity, 88% specificity, and 85% accuracy (►**Table 2**).

## Discussion

Our prospective study shows that USFF derived from multivariable QUS correlates strongly with MRI-PDFF ($r = 0.912$). These results align with the correlations reported by Jeon et al ($r = 0.799$–$0.824$) in 2023,[4] and are similar to earlier single-parameter QUS studies.[12–14]

Among three parameters, USFF exhibited the highest AUC for assessing MRI-PDFF ≥ 5%, ≥ 15%, and ≥ 25% (AUCs of 0.915, 0.995, and 0.991). These findings align with those reported by Jeon et al in 2023, who also found that USFF had the highest AUC values (0.905–0.956) for diagnosing hepatic steatosis across multiple MRI-PDFF thresholds.[4] USFF, derived from multivariable QUS, has an optimal cutoff of 9.1% for diagnosing hepatic steatosis (MRI-PDFF ≥ 5%), with a sensitivity of 88%, specificity of 80%, and overall accuracy of 85%. These findings align with those of Jeon et al in 2023, who reported a USFF cutoff of 8.7% that achieved over 95% specificity in their development cohort.[4]

The diagnostic performance of TAI and TSI in this study highlights the shift from qualitative visual assessment to objective, multiparametric quantification of hepatic steatosis. Our findings show that TAI, with a cutoff of 0.72 and 100% sensitivity, is an excellent screening tool for excluding liver fat. In contrast, TSI, with an AUC of 0.9093 and a high

 

**Table 1** Patient demographics and quantitative liver fat measurements assessed by ME-GRE MRI and ultrasound

| No. | Gender | Age | BMI | PDFF (%) | USFF (%) | TAI | | TSI | |
|---|---|---|---|---|---|---|---|---|---|
| | | | | Mean ± SD | | Mean | Median | Mean | Median |
| 1 | Female | 74 | 26.2 | 29.0 ± 1.9 | 28.59 | 1.15 | 1.15 | 105.12 | 105.27 |
| 2 | Female | 67 | 23.8 | 13.3 ± 2.7 | 14.20 | 0.82 | 0.82 | 102.74 | 103.90 |
| 3 | Male | 52 | 21.7 | 4.3 ± 0.7 | 13.33 | 0.79 | 0.81 | 104.39 | 105.51 |
| 4 | Female | 54 | 23.4 | 7.0 ± 0.2 | 8.57 | 0.72 | 0.72 | 96.60 | 98.29 |
| 5 | Male | 53 | 21.3 | 1.3 ± 0.3 | 0.0 | 0.56 | 0.56 | 74.03 | 74.71 |
| 6 | Female | 24 | 21.6 | 1.0 ± 0.3 | 0.0 | 0.59 | 0.60 | 90.34 | 92.74 |
| 7 | Female | 65 | 23.4 | 6.5 ± 0.8 | 10.98 | 0.74 | 0.74 | 103.28 | 104.89 |
| 8 | Male | 54 | 23.6 | 1.5 ± 1.1 | 0.0 | 0.49 | 0.51 | 86.65 | 86.71 |
| 9 | Male | 58 | 25.7 | 12.4 ± 1.9 | 13.59 | 0.82 | 0.83 | 100.14 | 101.72 |
| 10 | Female | 60 | 25.4 | 11.4 ± 1.0 | 15.20 | 0.83 | 0.84 | 100.44 | 100.30 |
| 11 | Female | 48 | 21.9 | 1.4 ± 0.5 | 0.0 | 0.55 | 0.56 | 76.65 | 76.64 |
| 12 | Male | 39 | 23.2 | 1.7 ± 0.7 | 0.0 | 0.57 | 0.58 | 76.33 | 76.74 |
| 13 | Female | 76 | 20.4 | 3.1 ± 0.7 | 13.68 | 0.82 | 0.82 | 100.54 | 102.38 |
| 14 | Male | 79 | 26.6 | 11.3 ± 1.6 | 17.11 | 0.86 | 0.86 | 107.97 | 108.11 |
| 15 | Female | 59 | 25.5 | 11.0 ± 2.0 | 15.51 | 0.84 | 0.84 | 104.73 | 103.66 |
| 16 | Male | 66 | 23.9 | 5.9 ± 0.7 | 9.10 | 0.73 | 0.72 | 96.14 | 95.56 |
| 17 | Female | 50 | 26.2 | 17.1 ± 1.5 | 15.97 | 0.85 | 0.85 | 104.93 | 104.52 |
| 18 | Male | 22 | 25.4 | 10.6 ± 0.8 | 15.26 | 0.83 | 0.84 | 105.44 | 105.30 |
| 19 | Male | 61 | 23.3 | 1.9 ± 0.5 | 0.0 | 0.52 | 0.52 | 74.99 | 74.51 |
| 20 | Female | 69 | 23.3 | 8.1 ± 1.9 | 11.86 | 0.74 | 0.74 | 104.93 | 105.39 |
| 21 | Male | 57 | 23.9 | 1.6 ± 0.7 | 0.0 | 0.58 | 0.57 | 82.79 | 82.96 |
| 22 | Female | 47 | 20.5 | 4.6 ± 0.6 | 9.08 | 0.74 | 0.74 | 95.88 | 94.07 |
| 23 | Female | 59 | 23.5 | 9.7 ± 1.0 | 10.02 | 0.73 | 0.73 | 100.98 | 99.48 |
| 24 | Female | 83 | 26 | 21.2 ± 2.0 | 28.82 | 1.15 | 1.14 | 106.09 | 106.80 |
| 25 | Female | 29 | 23.1 | 7.8 ± 1.0 | 12.99 | 0.8 | 0.81 | 101.15 | 99.22 |
| 26 | Female | 53 | 23.8 | 5.5 ± 0.5 | 11.17 | 0.79 | 0.78 | 95.17 | 94.90 |
| 27 | Female | 68 | 20.5 | 5.8 ± 1.8 | 9.14 | 0.73 | 0.72 | 97.74 | 95.56 |
| 28 | Female | 67 | 25.2 | 2.9 ± 0.5 | 8.82 | 0.76 | 0.76 | 90.54 | 89.60 |
| 29 | Male | 76 | 23.5 | 24.2 ± 1.1 | 25.07 | 1.05 | 1.04 | 107.99 | 107.67 |
| 30 | Female | 72 | 20.7 | 7.1 ± 1.0 | 9.05 | 0.74 | 0.74 | 95.08 | 94.07 |
| 31 | Female | 52 | 20.1 | 4.6 ± 0.2 | 9.11 | 0.73 | 0.72 | 97.14 | 95.56 |
| 32 | Female | 67 | 20.9 | 2.2 ± 0.2 | 5.53 | 0.64 | 0.64 | 97.92 | 97.33 |
| 33 | Female | 30 | 20.9 | 2.9 ± 1.5 | 10.41 | 0.76 | 0.77 | 97.29 | 98.81 |
| 34 | Male | 32 | 23.8 | 1.2 ± 0.5 | 0.0 | 0.53 | 0.52 | 72.78 | 72.40 |
| 35 | Female | 62 | 25.4 | 5.2 ± 0.4 | 11.24 | 0.73 | 0.73 | 106.2 | 105.42 |
| 36 | Male | 69 | 25.5 | 10.3 ± 0.2 | 15.06 | 0.85 | 0.86 | 101.04 | 100.50 |
| 37 | Female | 37 | 25.3 | 12.2 ± 1.4 | 15.86 | 0.85 | 0.85 | 104.88 | 104.41 |
| 38 | Female | 75 | 24.7 | 11.1 ± 1.2 | 15.54 | 0.84 | 0.84 | 104.78 | 103.66 |
| 39 | Male | 70 | 25.8 | 28.3 ± 2.5 | 29.95 | 1.16 | 1.16 | 107.87 | 107.46 |
| 40 | Female | 78 | 23.4 | 38.5 ± 1.9 | 30.86 | 1.19 | 1.18 | 107.67 | 107.65 |

Abbreviations: BMI, body mass index; ME-GRE, multi-echo gradient echo; MRI-PDFF, magnetic resonance imaging-proton density fat fraction; TAI, tissue attenuation imaging; TSI, tissue scatter distribution imaging; USFF, ultrasound fat fraction.

 

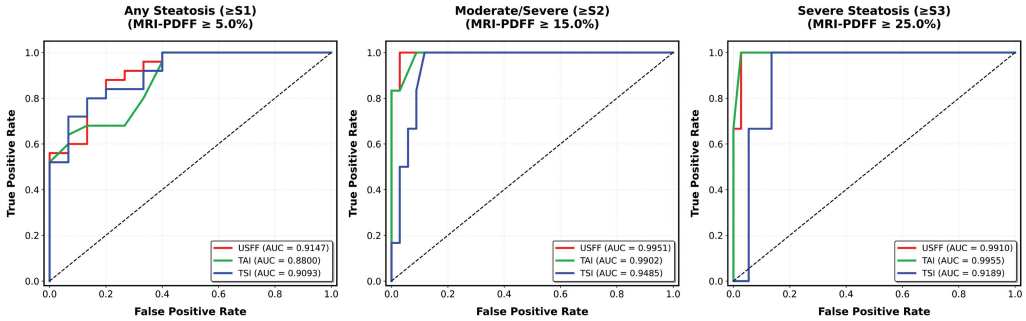


**Fig. 2** Receiver operating characteristic (ROC) curves showing the diagnostic performance of USFF for detecting PDFF thresholds of ≥5% (S1), ≥15% (S2), and ≥25% (S3). USFF demonstrated the highest area under the curve (AUC) across all thresholds, indicating superior diagnostic accuracy for hepatic fat quantification. MRI-PDFF, magnetic resonance imaging-proton density fat fraction; PDFF, proton density fat fraction.

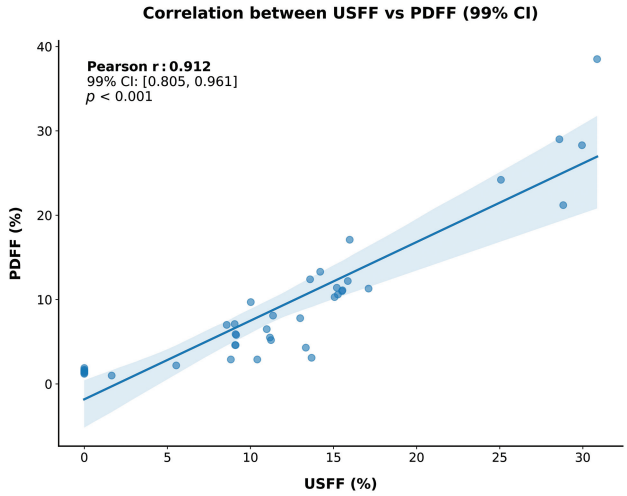


**Fig. 3** Correlation between USFF and MRI-PDFF with 95% confidence interval. A scatter plot showing a strong linear relationship between USFF and PDFF ($r = 0.912$; $p < 0.001$). The solid line indicates the line of best fit, and the gray-shaded area represents the 95% confidence interval. MRI-PDFF, magnetic resonance imaging-proton density fat fraction; USFF, ultrasound fat fraction.

specificity of 86.67%, offers superior diagnostic accuracy for confirming tissue changes. By capturing two different physical phenomena: (1) signal energy loss through TAI and (2) micro-architectural echo distribution via TSI, this dual-parameter approach overcomes the subjectivity associated with traditional B-mode ultrasound. USFF values, derived from the TSI and TAI indices, significantly enhance performance in classifying fatty liver disease, with all performance indices exceeding 0.800 (►**Table 2**). USFF demonstrated the highest AUC for detecting hepatic steatosis. Additionally, the 9.14% cutoff for USFF aligns with established MRI-PDFF thresholds, indicating that these ultrasound-derived biomarkers provide a reliable, non-invasive, and accessible alternative for early detection and ongoing monitoring of metabolic dysfunction-associated steatotic liver disease. Our TAI and TSI cut-off thresholds are similar to previous studies.[15–17]

USFF offers several practical advantages: (1) the examination is completed in seconds during a routine abdominal ultrasound, (2) the technique is widely available with minimal additional cost, (3) results are expressed as a percentage, making patient counseling and long-term follow-up easier, and (4) no ionizing radiation or intravenous contrast is necessary.[2,10] In resource-limited settings where MRI access is restricted, USFF can serve as a gatekeeper, reserving MRI or biopsy for indeterminate or complex cases.

Based on our study results, USFF demonstrated strong diagnostic accuracy for both the detection and grading of hepatic steatosis. Therefore, we believe that USFF can serve as a valuable adjunct to conventional B-mode ultrasound for screening and initial assessment of hepatic steatosis in clinical practice. Although liver biopsy remains the gold standard for histological staging, accumulating evidence indicates that MRI-PDFF can reliably replace biopsy for measuring fat. The high agreement between USFF and MRI-PDFF in our study further supports the clinical value of QUS as a primary, non-invasive test.

## Limitations

This study has several limitations. First, the sample size was relatively small, and the investigation was performed at a single center. The lack of histopathologic correlation prevented direct assessment of diagnostic accuracy compared with liver biopsy. Future multicenter studies with larger cohorts and histological confirmation are necessary to establish optimal USFF cut-off values for each steatosis grade. Additionally, liver stiffness was not measured using MRI or shear-wave elastography, and repeated USFF measurements over time were not conducted. Further research combining USFF with liver stiffness assessment is needed to provide a more comprehensive evaluation of hepatic steatosis and fibrosis and to verify USFF's potential for monitoring treatment responses to lifestyle changes or medication.

## Conclusion

Quantitative ultrasound fat fraction provides a rapid, cost-effective, and accurate method for detecting and assessing

 

**Table 2** Diagnostic performance of USFF, TAI, and TSI in identifying hepatic steatosis grade S1 (≥5%)

| Model | Cut-off | AUC | *p*-Value | Accuracy (95% CI) | Sensitivity (95% CI) | Specificity (95% CI) | PPV (95% CI) | NPV (95% CI) |
|---|---|---|---|---|---|---|---|---|
| USFF | 9.14 | 0.9147 | 0.0000 | 0.8500 (0.7093–0.9294) | 0.8800 (0.7004–0.9583) | 0.8000 (0.5481–0.9295) | 0.8800 (0.7004–0.9583) | 0.8000 (0.5481–0.9295) |
| TAI | 0.72 | 0.8800 | 0.0003 | 0.8500 (0.7093–0.9294) | 1.0000 (0.8668–1.0000) | 0.6000 (0.3575–0.8018) | 0.8065 (0.6372–0.9081) | 1.0000 (0.7009–1.0000) |
| TSI | 100.14 | 0.9093 | 0.0000 | 0.8250 (0.6805–0.9125) | 0.8000 (0.6087–0.9114) | 0.8667 (0.6212–0.9626) | 0.9091 (0.7219–0.9747) | 0.7222 (0.4913–0.8750) |

Abbreviations: AUC, area under the curve; CI, confidence interval; NPV, negative predictive value; PPV, positive predictive value; TAI, texture analysis index; TSI, tumor stiffness index; USFF, ultrasound feature fusion.

hepatic steatosis. Its strong correlation and high agreement with MRI-PDFF support incorporating USFF into routine ultrasound examinations and ongoing patient monitoring for those with or at risk of fatty liver disease.

### Ethical Approval

Institutional review board approval was obtained; all participants provided written informed consent.

### Data Availability Statement

Data are available upon request.

### Conflict of Interest

None declared.

### Acknowledgment

This work was supported by Hue University under the Core Research Program, Grant No. NCM.DHH.2020.09.

## References

1 Chau THT, Bannier E, Bardou-Jacquet E, Gandon Y. Liver R2* threshold to predict the failure of MR elastography at 3T: SE-EPI versus GRE sequences. Acta Radiol 2025;66(10): 1070–1076
2 Fetzer DTPT, Pierce TT, Robbin ML, et al. US quantification of liver fat: past, present, and future. Radiographics 2023;43(07): e220178
3 Grąt K, Grąt M, Rowiński O. Usefulness of different imaging modalities in evaluation of patients with non-alcoholic fatty liver disease. Biomedicines 2020;8(09):298
4 Jeon SK, Lee JM, Cho SJ, Byun YH, Jee JH, Kang M. Development and validation of multivariable quantitative ultrasound for diagnosing hepatic steatosis. Sci Rep 2023;13(01):15235
5 Kechagias S, Ekstedt M, Simonsson C, Nasr P. Non-invasive diagnosis and staging of non-alcoholic fatty liver disease. Hormones (Athens) 2022;21(03):349–368
6 Kim M, Kang BK, Jun DW. Comparison of conventional sonographic signs and magnetic resonance imaging proton density fat fraction for assessment of hepatic steatosis. Sci Rep 2018;8(01): 7759
7 Mancini M, Prinster A, Annuzzi G, et al. Sonographic hepatic-renal ratio as indicator of hepatic steatosis: comparison with (1)H magnetic resonance spectroscopy. Metabolism 2009;58(12): 1724–1730
8 Orcel T, Chau HT, Turlin B, et al. Evaluation of proton density fat fraction (PDFF) obtained from a vendor-neutral MRI sequence and MRQuantif software. Eur Radiol 2023;33(12): 8999–9009
9 Rodge GAGM, Goenka MK, Goenka U, Afzalpurkar S, Shah BB. Quantification of liver fat by MRI-PDFF imaging in patients with suspected non-alcoholic fatty liver disease and its correlation with metabolic syndrome, liver function test and ultrasonography. J Clin Exp Hepatol 2021;11(05):586–591
10 Ozturk A, Kumar V, Pierce TT, et al. The future is beyond bright: the evolving role of quantitative US for fatty liver disease. Radiology 2023;309(02):e223146
11 Park J, Lee JM, Lee G, Jeon SK, Joo I. Quantitative evaluation of hepatic steatosis using advanced imaging techniques: focusing on new quantitative ultrasound techniques. Korean J Radiol 2022;23 (01):13–29
12 Seen TKSM, Sayed M, Bilal M, et al. Clinical indicators for progression of nonalcoholic steatohepatitis to cirrhosis. World J Gastroenterol 2021;27(23):3238–3248

 

13 Wu S, Pan J, Song M, et al. Performance of magnetic resonance imaging and ultrasound for identifying the different degrees of hepatic steatosis: a systematic review and meta-analysis. Acad Radiol 2025;32(11):6528–6540
14 Siddiqui MSVR, Vuppalanchi R, Van Natta ML, et al; NASH Clinical Research Network. Vibration-controlled transient elastography to assess fibrosis and steatosis in patients with nonalcoholic fatty liver disease. Clin Gastroenterol Hepatol 2019;17(01):156–163.e2
15 Tada T, Kumada T, Toyoda H, et al. Utility of attenuation coefficient measurement using an ultrasound-guided attenuation parameter for evaluation of hepatic steatosis: comparison with MRI-determined proton density fat fraction. AJR Am J Roentgenol 2019;212 (02):332–341
16 Teng MLNC, Ng CH, Huang DQ, et al. Global incidence and prevalence of nonalcoholic fatty liver disease. Clin Mol Hepatol 2023;29(Suppl):S32–S42
17 Wibulpolprasert P, Subpinyo B, Chirnaksorn S, et al. Correlation between magnetic resonance imaging proton density fat fraction (MRI-PDFF) and liver biopsy to assess hepatic steatosis in obesity. Sci Rep 2024;14(01):6895

 